(19) Europäisches Patentamt
European Patent Office
Office européen des brevets

(11) **EP 2 976 017 B1**

(12) **EUROPEAN PATENT SPECIFICATION**

(45) Date of publication and mention of the grant of the patent:
02.10.2019 Bulletin 2019/40

(21) Application number: **14713923.2**

(22) Date of filing: **12.03.2014**

(51) Int Cl.:
A61B 8/08 *(2006.01)*

(86) International application number:
PCT/IB2014/059657

(87) International publication number:
WO 2014/147517 (25.09.2014 Gazette 2014/39)

(54) BEAMFORMING TECHNIQUES FOR ULTRASOUND MICROCALCIFICATION DETECTION

STRAHLENBÜNDELUNGSTECHNIKEN ZUM ULTRASCHALLNACHWEIS VON MIKROVERKALKUNGEN

TECHNIQUES DE FORMATION DE FAISCEAU POUR DÉTECTION DE MICROCALCIFICATIONS PAR ULTRASONS

(84) Designated Contracting States:
AL AT BE BG CH CY CZ DE DK EE ES FI FR GB GR HR HU IE IS IT LI LT LU LV MC MK MT NL NO PL PT RO RS SE SI SK SM TR

(30) Priority: **20.03.2013 US 201361803634 P**
21.11.2013 US 201361907022 P

(43) Date of publication of application:
27.01.2016 Bulletin 2016/04

(73) Proprietor: **Koninklijke Philips N.V.**
5656 AE Eindhoven (NL)

(72) Inventors:
- **ROBERT, Jean-luc**
  NL-5656 AE Eindhoven (NL)
- **HUANG, Sheng-Wen**
  NL-5656 AE Eindhoven (NL)
- **RADULESCU, Emil George**
  NL-5656 AE Eindhoven (NL)
- **VIGNON, Francois Guy Gerard Marie**
  NL-5656 AE Eindhoven (NL)
- **ERKAMP, Ramon Quido**
  NL-5656 AE Eindhoven (NL)

(74) Representative: **Steffen, Thomas**
Philips Intellectual Property & Standards
High Tech Campus 5
5656 AE Eindhoven (NL)

(56) References cited:
US-A1- 2006 171 573 **US-A1- 2009 247 869**

- **I. CHRISTOYIANNI ET AL: "Computer aided diagnosis of breast cancer in digitized mammograms", COMPUTERIZED MEDICAL IMAGING AND GRAPHICS, vol. 26, no. 5, 2 September 2002 (2002-09-02), pages 309-319, XP055131857, ISSN: 0895-6111, DOI: 10.1016/S0895-6111(02)00031-9**
- **SHENG-WEN HUANG ET AL: "Ultrasonic computed tomography reconstruction of the attenuation coefficient using a linear array", IEEE TRANSACTIONS ON ULTRASONICS, FERROELECTRICS AND FREQUENCY CONTROL, IEEE, US, vol. 52, no. 11, 2 November 2005 (2005-11-02), pages 2011-2022, XP011367532, ISSN: 0885-3010, DOI: 10.1109/TUFFC.2005.1561670**

EP 2 976 017 B1

Description

FIELD OF THE INVENTION

[0001] The present invention relates to medical imaging for identifying microcalcifications and, more particularly, to use of ultrasound as the imaging modality.

BACKGROUND OF THE INVENTION

[0002] Mammography's success for screening for breast cancer is mostly attributed to its capability for reliably imaging calcifications, an important marker for early stage breast cancer. Microcalcifications are present in 60-80% of breast cancers and are a reliable indicator of both benign and malignant lesions. The key diagnostic features of microcalcifications are their location, number, size, morphology, distribution, pattern, and relation to a mass. These features help stratify the risk of malignancy and often are the only marker of cancer. A relevant example is Ductal Carcinoma in Situ (DCIS), which accounts for 20% of breast cancers.

[0003] The article "Computer aided diagnoses of breast cancer in digitized mammograms", written by I. Christoyianni, Computerized Medical Imaging and Graphics, vol. 26, no.5, 1 September 2002, pages 309-319, XP055131857, ISSN: 0895-6111, discloses the implementation of a CAD system for breast cancer recognition that is capable of pinpointing regions of suspicions in digital mammograms. Independent component analysis has been used being capable of distinguishing between tumourous and healthy tissue.

[0004] US2006/0171573 A1 disloses the use of computer aided detection (CAD) system output diplays for providing accurate representations of areas for subsequent exams. In digital mammogram images clustered microcalcifications are detected. The clustered microcalcifications are classified and displayed. The CAD System outputs are used to improve the sensitivity and specificity for detection of regions associated with cancer.

[0005] However, mammography shows poor performance in dense breast tissue, the non-fatty portion of the breast. Dense breast tissue is more commonly found in younger women, and women in certain localities, China for example.

[0006] Also, despite measures to reduce the dose, mammography exposes the patient to ionizing radiation. In addition, there is the issue of patient comfort due to the need for compression plates.

[0007] The major limitation of conventional ultrasound, which is non-ionizing and needs no compression plates, is its poor sensitivity to microcalcifications. The sensitivity to microcalcifications is within 50-80%. The article "Ultrasonic computed tomography reconstruction of the attenuation coefficient using a linear array" written by Sheng-Wen Huang et al., IEEE Transactions on ultrasonics, ferroelectrics and frequency control, IEEE, US, vol. 52, no. 11, 1 November 2005, pages 2011-2022, discloses that in addition to conventional B-mode ultrasound, the sound velocity distribution and the attenuation coefficient distrubution in the breast can be used in diagnoses because the sound velocity is higher in cancerous tissue than in fat, and the attenuation coefficient ins higher in cancerous tissue than in a cyst. A reconstruction method for the attenuation coefficient distribution has been disclosed based on the angular spectrum method and the reconstructed sound velocity distribution.

[0008] Mallart discloses phase aberration correction of an ultrasonic transmit beam for the inhomogeneities of a medium through the use of a receive focusing criterion that is independent of both the scattering cross-section of the medium and the transmitted energy. See R. Mallart and M. Fink, "Adaptive focusing in scattering media through sound-speed inhomogeneities: The van Cittert Zernike approach and focusing criterion," J. Acoust. Soc. Am., vol. 96, no. 6, pp. 3721-3732, 1994.

SUMMARY OF THE INVENTION

[0009] What is proposed herein below is directed to addressing one or more of the above concerns.

[0010] Channel data contain much more information than B-mode images obtained after ultrasound receive beamforming. Therefore, channel-data-based beamforming techniques can provide better sensitivity and/or specificity for micro calcification detection than image processing techniques. The novel technology proposed herein enhances the contrast between microcalcifications and the background, i.e., body tissue in which the calcifications reside, typically soft tissue such as dense breast tissue.

[0011] In addition to the advantages noted above in using ultrasound for early-stage breast cancer detection, the screening and follow-up diagnostic procedures will be greatly simplified due to medical evaluation using only one modality. Also, good sensitivity to microcalcifications will facilitate easier identification of tumor location in ultrasound-guided biopsies, improving the workflow and diagnostic confidence.

[0012] In accordance with what is proposed herein, a medical ultrasound acquisition-data analysis device having channels is configured for: acquiring channel data via ultrasound received on the channels; using the acquired channel data to estimate coherence of the data and to derive dominance of an eigenvalue of a channel covariance matrix; and,

based on the estimate and the derived dominance, distinguishing microcalcifications from background.

[0013] A computer readable medium according to independent claim 24 is also provided.

[0014] Details of the novel, ultrasonic microcalcification identification technology are disclosed below with the aid of the following drawing, which is not drawn to scale, and the following formula sheet and flow charts.

BRIEF DESCRIPTION OF THE DRAWINGS

[0015]

Fig. 1 is a schematic diagram of an ultrasonic microcalcification identification device in accordance with the present invention;

Fig. 2 is a set of exemplary mathematical definitions and relationships in accordance with the present invention; and Figs. 3A-3D, 4A-4C, and 5 are flow charts of an exemplary ultrasonic microcalcification identification process in accordance with the present invention.

DETAILED DESCRIPTION OF EMBODIMENTS

[0016] FIG. 1 depicts, by way of illustrative and non-limitative example, a medical ultrasound acquisition-data analysis device characterizable as an ultrasonic microcalcification identification device 100.

[0017] The device 100 includes an ultrasound imaging probe 102 having an array 104 of transducer elements 106. The probe 102 is shown as pressed into acoustic contact with breast tissue 107.

[0018] The device 100 further includes channels 108 in connection with the elements 106. The channels have respective sample delay elements 110. The latter connect to a coherent summer 112, the summer and the receive delay elements 110 together constituting a receive beamformer 114. The delay elements 110 may be augmented to also provide amplitude weighting. Delay elements for steering and focusing transmit beams 116, 118 can be implemented and are not shown. The multiple transmit beams 116, 118 may be parallel, or may be differently angled, i.e., steered.

[0019] Also included in the device 100 are a coherence factor (CF) determination module 120, an eigenvalue dominance determination module 122, a microcalcification identification module 124, a signal and image processor 126, a display 128, and a scanning controller 130. The controller 130 controls the scanning as indicated by the oppositely-oriented scanning directional arrows 132, 134 in Fig. 1, and the other components of the device 100 shown in Fig. 1.

[0020] The beamforming strategy for microcalcification detection is to involve channel-data-based parameters that favor point targets 136, smaller than a spatial resolution, such as the lateral resolution 138 at that imaging depth 140. Microcalcifications 142 resemble such targets 136 acoustically.

[0021] The microcalcification 142 is the dominant scatterer in its resolution cell and causes isotropic scattering. A coherence factor and an eigenvalue dominance criterion, both discussed herein below, are utilized to respectively assess the isotropic scattering and the dominance of the microcalcification. In the background tissue there is no such dominance of a single, isotropic scatterer.

[0022] Two parts of a bifurcated approach proposed herein accordingly are coherence estimation using multiple transmit beams and covariance matrix analysis to extract eigenvalues.

[0023] More generally, it is noted at the outset that channel data, after applying beamforming delays but before coherent summing, i.e., "post-delay channel data", 144 is outputted by the summer 112. This is complex data generally in the form "a+bi", as shown in Fig. 1, i.e., such that both the real and imaginary components of a datum can be nonzero. The channel data 144 is routed to the eigenvalue dominance determination module 122. The same data 144 is routable to the CF module 120 for summing there, although summing can alternatively, or in addition, be performed in the summer 112 as seen from the alternative path 145 in Fig. 1. Also, the beamforming done by the CF module 120 can stand alone in forming field points for further image processing in the signal and image processor 126. Or, alternatively or in addition, summed output of the summer 112, which may for example be subject, in the summer, to amplitude weighting, can be submitted for processing by the signal and image processor 126. In either event, the signal and image processor 126 prepares the beamformed data for display, performing functions such as frequency compounding, logarithic compression and scan conversion.

[0024] Referring now to the first part of the bifurcated approach, coherence estimation, let $S(m,n,tx,rx)$ denote complex RF channel data (or "delayed data") 144, i.e., after applying beamforming delays and optionally amplitude weighting. Here, m is the imaging depth/time counter or index, n the channel index, tx the transmit beam index, and rx the receive beam index. A coherence factor (CF) or "focusing criterion" at a spatial point (m,rx), or field point, 146 with a single transmit beam 116 is:

$$CF_0(m,rx) \equiv \frac{|\sum_{n=1}^{N} S(m,n,rx,rx)|^2}{N\sum_{n=1}^{N}|S(m,n,rx,rx)|^2} = \frac{\left|\frac{1}{N}\sum_{n=1}^{N} S(m,n,rx,rx)\right|^2}{\frac{1}{N}\sum_{n=1}^{N}|S(m,n,rx,rx)|^2},$$

where N is the number of channels 108. The term $\left|\frac{1}{N}\sum_{n=1}^{N} S(m,n,rx,rx)\right|^2$ is denoted as $I_c(m,rx)$, where the subscript "c" stands for coherent, as it can be interpreted as the average coherent intensity over channels at the point (m,rx). The denominator on the right can be expressed as

$$\frac{1}{N}\sum_{n=1}^{N}|S(m,n,rx,rx)|^2 = \frac{1}{N}\sum_{n=1}^{N}|\Delta S(m,n,rx,rx)|^2 + \left|\frac{1}{N}\sum_{n=1}^{N} S(m,n,rx,rx)\right|^2$$

where

$$\Delta S(m,n,rx,rx) = S(m,n,rx,rx) - \frac{1}{N}\sum_{n=1}^{N} S(m,n,rx,rx).$$

[0025] The term $\frac{1}{N}\sum_{n=1}^{N}|\Delta S(m,n,rx,rx)|^2$ is denoted as $I_{inc}(m,rx)$, where the subscript "inc" stands for incoherent. This is because $I_{inc}(m,rx)$ reflects the average intensity of incoherent signals (in the surroundings of (m,rx) decided by the focusing quality on transmit) and is zero when the channel data 144 are fully coherent. Substituting terms,

$$CF_0(m,rx) = \frac{I_c(m,rx)}{I_{inc}(m,rx) + I_c(m,rx)} = \frac{1}{\frac{I_{inc}(m,rx)}{I_c(m,rx)} + 1}.$$

[0026] Therefore, $CF_0(m,rx)$ indicates how much the point (m,rx) is brighter than its surroundings. CF_0 ranges between 0 and 1 and it reaches the maximum 1 if and only if the channel data 144 are fully coherent. Full coherence means that $S(m,1,rx,rx) = S(m,2,rx,rx) = \cdots = S(m,N,rx,rx)$. Around a strong point target or a reflector, the CF_0 value is high.

[0027] To distinguish point targets, which microcalcifications 142 in background tissue 148 resemble acoustically, from planar reflectors, multiple transmit beams 116, 118 can be incorporated into CF estimation. CF is thereby redefinable as:

$$CF(m,rx) \equiv \frac{\sum_{tx=rx-\Delta}^{rx+\Delta}\left|\sum_{n=1}^{N} S(m,n,tx,rx)\right|^2}{\sum_{tx=rx-\Delta}^{rx+\Delta} N\sum_{n=1}^{N}|S(m,n,tx,rx)|^2} \qquad \text{(definition 1)}$$

which definition, like the ones that follow, is repeated in Fig. 2.

[0028] As mentioned above, the spatial point (m,rx) 146 is a function of both an associated receive beam rx 150 and a spatial depth 140 or time. The estimating operates on the delayed data 144 by summing, thereby performing beamforming. The $CF(m,rx)$ estimate, or result of the estimating, 204 includes spatial compounding of the CF by summing, over multiple transmit beams 116, 118, a squared-magnitude function 206 and a squared beamsum 208, i.e. summed result of beamforming. The function 206 and beamsum 208 are both formed by summing over the channels 108.

[0029] Referring now to the second part the bifurcated approach, let $\mathbf{R}(m,rx)$ denote a covariance matrix, or "correlation/covariance matrix", 210 at the point (m,rx) obtained by temporal averaging over a range 214 of time or spatial depth 140:

$$\mathbf{R}(m,rx) \equiv \frac{1}{2d+1}\sum_{p=m-d}^{m+d}\mathbf{s}(p,rx)\mathbf{s}^{\mathrm{H}}(p,rx) \qquad \text{(definition 2)}$$

where

$$\mathbf{s}(p,rx)=\begin{bmatrix}S(p,1,rx,rx)\\S(p,2,rx,rx)\\\vdots\\S(p,N,rx,rx)\end{bmatrix}. \qquad \text{(definition 3)}$$

[0030] As R(m, *rx)* is positive semidefinite, all of its eigenvalues 212 are real and nonnegative. Denote the eigenvalues by $\{\gamma_i(m,rx)\}_{i=1}^{N}$ with $\gamma_i \geq \gamma_{i+1}$. Then the trace of **R**(*m*,*rx*) is

$$\mathrm{Tr}\{\mathbf{R}(m,rx)\}\equiv\sum_{i=1}^{N}\mathbf{R}_{ii}(m,rx)=\sum_{i=1}^{N}\gamma_i(m,rx). \qquad \text{(definition 4)}$$

[0031] The dominance 216 of the first eigenvalue 218 is represented as

$$\mathrm{ev_d}(m,rx)\equiv\frac{1}{1-\frac{\gamma_1(m,rx)}{\mathrm{Tr}\{\mathbf{R}(m,rx)\}}}. \qquad \text{(definition 5)}$$

[0032] It is infinite if $\gamma_i(m,rx) = 0$ for $i \geq 2$ (i.e., if the rank of **R**(*m*,*rx*) is 1) as Tr{**R**(*m*,*rx*)} = $\gamma_1(m,rx)$, and finite otherwise. Summing over several transmits 116, 118 (beam averaging) could also be applied in correlation matrix analysis, as follows:

$$\mathbf{R}(m,rx)\equiv\frac{1}{(2d+1)(2g+1)}\sum_{p=m-d}^{m+d}\sum_{tx=rx-g}^{rx+g}\mathbf{s}(p,tx,rx)\mathbf{s}^{\mathrm{H}}(p,tx,rx) \qquad \text{(definition 6)}$$

where

$$\mathbf{s}(p,tx,rx)=\begin{bmatrix}S(p,1,tx,rx)\\S(p,2,tx,rx)\\\vdots\\S(p,N,tx,rx)\end{bmatrix} \qquad \text{(definition 7)}$$

[0033] Another way of combining transmits is to form the covariance matrix from data generated by an algorithm that recreates focused transmit beams retrospectively. An example utilizing retrospective dynamic transmit (RDT) focusing is as follows, and, for other such algorithms such as plane wave imaging (see G. Montaldo, M. Tanter, J. Bercoff, N. Benech, and M. Fink, "Coherent plane-wave compounding for very high frame rate ultrasonography and transient elastography," IEEE Trans. Ultrason. Ferroelectr. Freq. Control, vol. 56, no. 3, pp. 489-506, 2009) and synthetic aperture beamforming (see J. A. Jensen, S. I. Nikolov, K. L. Gammelmark, and M. H. Pedersen, "Synthetic aperture ultrasound imaging," Ultrasonics, vol. 44, supplement, pp. e5-e15, 2006), analogous eigenvalue dominance computations apply:

$$\mathbf{R}(m,rx)\equiv\frac{1}{2d+1}\sum_{p=m-d}^{m+d}\mathbf{s}_{\mathrm{RDT}}(p,rx)\mathbf{s}_{\mathrm{RDT}}^{\mathrm{H}}(p,rx)$$

where

$$\mathbf{s}_{\mathrm{RDT}}(p,rx) = \begin{bmatrix} S_{\mathrm{RDT}}(p,1,rx) \\ S_{\mathrm{RDT}}(p,2,rx) \\ \vdots \\ S_{\mathrm{RDT}}(p,N,rx) \end{bmatrix},$$

and $S_{\mathrm{RDT}}(p,n,rx)$ are the dynamically transmit-beamformed complex RF channel data obtained by performing retrospective dynamic transmit (RDT) focusing on the original channel data $S(m,n,tx,rx)$. See U.S. Patent No. 8,317,712 to Burcher et al.

[0034] In the above bifurcated approach, $CF_0(m,rx)$ or $CF(m,rx)$ can, as with the dominance, likewise be obtained by temporal averaging over a range 214 of time or spatial depth 140. Coherence factor can also be estimated using dynamically transmit-beamformed channel data as follows:

$$CF_{\mathrm{RDT}}(m,rx) \equiv \frac{|\sum_{n=1}^{N} S_{\mathrm{RDT}}(m,n,rx)|^2}{N\sum_{n=1}^{N}|S_{\mathrm{RDT}}(m,n,rx)|^2}.$$

[0035] According to J.R. Robert and M. Fink, "Green's function estimation in speckle using the decomposition of the time reversal operator: Application to aberration correction in medical imaging," J. Acoust. Soc. Am., vol. 123, no. 2, pp. 866-877, 2008, the dominance of the first eigenvalue $ev_d(m,rx)$ can be approximated by $1/(1-CF_1(m,rx))$, where $CF_1(m,rx)$ is a coherence factor obtained from channel data $S(m,n,tx,rx)$. Temporal averaging 230, averaging over multiple transmit beams 116, 118, and/or RDT can be applied in calculating $CF_1(m,rx)$. Inversely, coherence factor can be approximated by eigenvalue dominance derived with proper averaging.

[0036] Figs. 3A-3D relate to the portion of the ultrasonic microcalcification identification process up until metric calculation. The procedure described below is an example of live, dynamic, real-time imaging, although it can be simplified to return a single B-mode image bearing the distinguished calcifications.

[0037] In accordance with a scanning process 302, shown in Fig. 3A, transmits 116, 118 are issued (step S302). This can be done serially on transmit in a range around the center 152 of the receive beam 150 using for example RDT scanning sequences. For each transmit there can be multiple receive beams, leading to multiple transmits per receive beam. Or a single transmit 116 may be issued per receive beam 150 as is done for the estimating of $CF_0(m,rx)$, the estimate without beam averaging. In the case of a single transmit or in the case of multiple ones, for each transmit there is a receive, via the receive beam 150 (step S304) or there are multiple receives. The transmits 116 and receives 150 proceed, until scanning is complete or otherwise halted (step S306).

[0038] A concurrent channel data acquisition subprocess 304, shown in Fig. 3B, acquires complex channel data (step S308), and delays the data samples by channel (step S310). This occurs repeatedly, until scanning is complete or otherwise halted (step S312).

[0039] In a concurrent coherence factor estimation subprocess 306, seen in Fig. 3C, samples that vary by channel are obtained (step S314). They are coherently summed, thereby completing a beamforming procedure (step S316). The magnitude of each sample is calculated channel by channel (step S318). If there exists a next transmit 116, for beam averaging, for the current spatial point 146 being interrogated (step S320), a transmit counter is incremented (step S322), and processing returns to the sample-obtaining step S314. Otherwise, if there does not exist a next transmit 116 (step S320), the transmit counter is reset (step S324). Summation for beamforming and summation of sample magnitudes are performed over all transmits 116 for the current spatial point 146 (step S326). The coherence factor CF 204 is computed (step S328).

[0040] Meanwhile, in a concurrent dominance derivation subprocess 308 of Fig. 3D, samples are obtained that vary by channel (step S330). A conjugate transpose 220 of a column matrix of the samples ordered by channel is formed (step S332). A product 222 is taken of the two matrices (step S334). If a next transmit 116, for beam averaging, exists for the current spatial point 146 (step S336), the transmit counter is incremented (step S338) and processing returns to the sample acquisition step S330. Otherwise, if a next transmit 116 does not exist (step S336), the transmit counter is reset (step S340). Query is then made as to whether a next neighbor point 224 for temporal averaging exists (step S342). If a next neighbor point 224 exists (step S342), the neighbor point counter is incremented (step S346) and processing returns to the sample acquisition step S330. Otherwise, if a next neighbor point 224 does not exist (step S342), the neighbor counter is reset (step S348). The product matrix from step S334 is summed over the transmits 116 and neighbor points 224 (step S350). As seen from definition 2 in Fig. 2, a covariance matrix with beam averaging 226 is computed based on the summed products 222 (step S352). A set of eigenvalues 212 are computed for the covariance matrix 226 by methods well known in the art (step S354). The largest 218 from among the eigenvalues is found (step S356). It is compared 228 with the set (step S358). The dominance 216 is calculated (step S360).

[0041] The estimation and derivation subprocesses 306, 308 are executed in the context of scanning subprocess 402 which is presented in Fig. 4A. In a first step, a metric is computed for the current spatial point 146 (step S402). Step S402 corresponds to either the estimation or derivation subprocess 306, 308. Accordingly, both the coherence factor (CF) determination module 120 and the eigenvalue dominance determination module 122 invoke the instant scanning subprocess 402. If time, rather than spatial depth, is being indexed for temporal tracking (step S404), and a next time exists for the current receive beam 150 (step S406), the time counter is incremented (step S408) and return is made to step S402. Likewise, if, instead of time, spatial depth is being indexed for temporal tracking (step S404), and a next spatial depth exists for the current receive beam 150 (step S410), the spatial depth counter is incremented (step S414) and return is made to step S402. If, on the other hand, no next time or spatial depth exists (steps S406, S410), correspondingly the time or spatial depth counter is reset (steps S416, S418). If, at this juncture, a next receive beam 150 exists in the current frame or scan (step S420), the receive beam counter is incremented (step S422). Otherwise, if no next receive beam 150 exists (step S420), the receive counter is reset (S424). If a next frame exists (step S425), processing points to the next frame (step S426) and return is made to the metric computation step S402.

[0042] The microcalcification identification module 124 concurrently executes a first version 404 of a microcalcification mapping subprocess, shown in Fig. 4B. First, the CF 204 and the dominance 216 are combined, as by multiplication (step S427). If the product is large enough to meet a combination threshold (step S428), the respective (and current) spatial point 146 is added to the microcalcification map for the current imaging frame (step S430). A microcalcification 142 has therefore been distinguished from background 148. If there is a next point in the frame (step S432), processing points to that next point (step S434) and return is made to the start of the subprocess 404. Otherwise, if there is no next point in the current frame (step S432), but there is a next frame to process (step S436), processing points to the next point (step S434) and return is made to the start of the subprocess 404.

[0043] Alternatively or in addition, the microcalcification identification module 124 concurrently executes a second version 406 of a microcalcification mapping subprocess, as seen from Fig. 4C. If a first coherence threshold is met, i.e., the CF 204 is large enough to meet it (step S440), the current spatial point 146 is added to the microcalcification map for the current imaging frame (step S442). On the other hand, even if the first coherence threshold is not met (step S440), but the CF 204 is large enough to meet another, i.e., second, predetermined coherence threshold (step S444) and the dominance 216 is large enough to meet a dominance threshold (step S446), the current spatial point 146 is added to the microcalcification map (step S442). If a next point exists in the current frame (step S448), processing points to that next point (step S450) and return is made to step S440. If, on the other hand, with the first coherence threshold not being met (step S440), if either the second coherence threshold or dominance threshold is likewise not met or both are not met (steps S444, S446), and if a next point exists (step S448), processing points to that next point (step S450) and return in made to step S440. In any event, when no next point in the current frame exists (step S448), if a next frame exists (step S452), processing points to that next frame (step S454) and return is made to step S440.

[0044] The microcalcification identification module 124 is also concurrently invoking a visual calcification discrimination subprocess 502, represented in Fig. 5. To the current frame for display, the corresponding microcalcification map is applied (step S502). All spatial points 146, e.g., voxels, in the current frame have been processed in either the first or second versions 404, 406 of the microcalcification mapping subprocess. The entries of the current microcalcification map denote microcalcifications 142 and are to be distinguished visually for presentation on-screen (step S504). This is done by highlighting, coloring or distinctive coloring, annotation with labels and/or screen pointers, etc., and is done by means of overlays, the adjustment of grey level, or any other known and suitable means. The image bearing the distinguished calcifications is displayed (step S506). If a next frame exists (step S508), processing points to that next frame (step S510), and returns to the map application step S502.

[0045] A medical ultrasound acquisition-data analysis device acquires channel data via ultrasound received on the channels, uses the acquired channel data to estimate data coherence and derive dominance of an eigenvalue of a channel covariance matrix and, based on the estimate and dominance, distinguishes microcalcifications from background. Microcalcifications may then be made distinguishable visually onscreen via highlighting, coloring, annotation, etc. The channel data operable upon by the estimating may have been subject to beamforming delays and may be summed in a beamforming procedure executed in the estimating. In the estimating and deriving, both field point-by-field point, multiple serial transmits may be used for each field point. In one embodiment results of the estimating and deriving are multiplied point-by-point and submitted to thresholding.

[0046] While the invention has been illustrated and described in detail in the drawings and foregoing description, such illustration and description are to be considered illustrative or exemplary and not restrictive; the invention is not limited to the disclosed embodiments.

[0047] For example, within the intended scope of what is proposed herein is a computer readable medium, as described below, such as an integrated circuit that embodies a computer program having instructions executable for performing the subprocesses 306, 308, 404, 406, 502 described above for microcalcification discrimination. The functions are implementable by any combination of software, hardware and firmware.

[0048] A computer program can be stored momentarily, temporarily or for a longer period of time on a suitable computer-

readable medium, such as an optical storage medium or a solid-state medium. Such a medium is non-transitory only in the sense of not being a transitory, propagating signal, but includes other forms of computer-readable media such as register memory, processor cache, RAM and other volatile memory.

[0049] A single processor or other unit may fulfill the functions of several items recited in the claims. The mere fact that certain measures are recited in mutually different dependent claims does not indicate that a combination of these measures cannot be used to advantage.

Claims

1. A medical ultrasound acquisition-data analysis device having a plurality of channels (108) and configured for:

   acquiring channel data via ultrasound received on the channels;
   characterized in that the acquired channel data are used to estimate coherence of said data and to derive dominance of an eigenvalue of a channel covariance matrix; and,
   based on the estimate and the derived dominance, distinguishing microcalcifications (142) from background.

2. The device of claim 1, comprising a display (128) and further configured for displaying, on said display, the distinguished microcalcifications in an ultrasound view.

3. The device of claim 2, further configured for displaying on said display, said microcalcifications in a presentation that, based on a result of said distinguishing, visually discriminates (S504) said microcalcifications from said background.

4. The device of claim 1, said using comprising using said data (144) to estimate coherence of said data individually with respect to a plurality of spatial points having respectively both a) an associated receive beam; and b) a spatial depth or time.

5. The device of claim 4, said using further comprising using said channel data in the deriving (S360) separately by point with respect to the plural points.

6. The device of claim 4, further configured for combining (S427) the estimates and the derivations point-by-point for said plurality of points.

7. The device of claim 6, said combining comprising multiplying said estimates by said derivations point-by-point for said plurality of points (146).

8. The device of claim 6, said combining yielding respective values, said device being further configured for thresholding (S428) said values, output of said thresholding spatially identifying said microcalcifications.

9. The device of claim 1, said estimating comprising spatial compounding of a coherence factor (204) by summing, over multiple transmit beams, a function of said data with respect to: a) a given receive beam; and b) a given spatial depth or time.

10. The device of claim 9, said estimating (306) further comprising summing said function over said channels.

11. The device of claim 1, further configured for a datum from among said acquired channel data being complex, with its real and imaginary parts both being nonzero, upon use for the estimating and for the deriving, said data, upon said use, having been subject to beamforming delays (S310).

12. The device of claim 1, said using comprising subjecting the acquired channel data to beamforming delays.

13. The device of claim 12, said device being further configured such that the estimating operates on the delayed data by summing, thereby performing beamforming (145).

14. The device of claim 12, said device being further configured such that the deriving operates on the delayed data separately by channel.

15. The device of claim 1, said matrix (210) having a plurality of eigenvalues, said eigenvalue being among the plural eigenvalues, said dominance being a metric representing a comparison between said eigenvalue and said plural eigenvalues, said device being configured for creating said matrix from said acquired channel data, said deriving comprising computing said eigenvalue.

16. The device of claim 1, said channel data being, upon said deriving, complex radiofrequency channel data to which beamforming delays have been applied, said deriving comprising taking a conjugate transpose (220) of a matrix of said channel data, entries of said conjugate transpose varying by channel.

17. The device of claim 16, said deriving comprising:

forming a product matrix, said forming comprising multiplying said matrix of said channel data by said conjugate transpose; and
averaging said product matrix over a range of spatial depth (140) or time to derive said dominance corresponding to a given spatial point.

18. The device of claim 16, said deriving comprising:

forming a product matrix, said forming comprising multiplying said matrix (222) of said channel data by said conjugate transpose; and
averaging said product matrix over multiple transmits.

19. The device of claim 16, configured for, in creating said complex radiofrequency channel data, using an algorithm that recreates focused transmit beams retrospectively.

20. The device of claim 1, said distinguishing comprising deciding (S440), based on application of a coherence threshold to a result of the estimating, that a microcalcification resides at a given spatial point.

21. The device of claim 20, said distinguishing comprising checking, if the decision is other than that a microcalcification resides at the given spatial point, whether said result and said derived dominance respectively meet another coherence threshold and a dominance threshold (S444, S446).

22. The device of claim 1, said acquiring for a microcalcification particle being performed with a spatial resolution (138), said particle being smaller than said resolution.

23. The device of claim 1, said background being body tissue (107) which said microcalcifications reside.

24. A computer readable medium embodying a program for medical ultrasound acquisition-data analysis, said program having instructions executable by a processor for causing the device of claim 1 to perform the following acts:

acquiring channel data via ultrasound received on multiple channels;
using the acquired channel data to estimate coherence of said data and to derive dominance of an eigenvalue (212) of a channel covariance matrix; and,
based on the estimate and the derived dominance, distinguishing microcalcifications from background.

Patentansprüche

1. Vorrichtung zur Analyse von medizinischen Ultraschallerfassungsdaten mit einer Vielzahl von Kanälen (108) und konfiguriert zum:

Erfassen von Kanaldaten über auf den Kanälen empfangenen Ultraschall; **dadurch gekennzeichnet, dass** die erfassten Kanaldaten verwendet werden, um die Kohärenz der genannten Daten zu schätzen und um die Dominanz eines Eigenwerts einer Kanalkovarianzmatrix abzuleiten; und
Unterscheiden von Mikroverkalkungen (142) vom Hintergrund basierend auf der Schätzung und der abgeleiteten Dominanz.

2. Vorrichtung nach Anspruch 1, umfassend eine Anzeige (128) und ferner konfiguriert zum Anzeigen der unterschie-

denen Mikroverkalkungen in einer Ultraschallansicht auf der genannten Anzeige.

3. Vorrichtung nach Anspruch 2, ferner konfiguriert zum Anzeigen der genannten Mikroverkalkungen auf der genannten Anzeige in einer Darstellung, die basierend auf einem Ergebnis der genannten Unterscheidung die genannten Mikroverkalkungen visuell von dem genannten Hintergrund abhebt (S504).

4. Vorrichtung nach Anspruch 1, wobei das genannte Verwenden das Verwenden der genannten Daten (144) zum individuellen Schätzen der Kohärenz der genannten Daten in Bezug auf eine Vielzahl von räumlichen Punkten mit jeweils sowohl a) einem zugehörigen Empfangsstrahlenbündel und b) einer räumlichen Tiefe oder Zeit umfasst.

5. Vorrichtung nach Anspruch 4, wobei das genannte Verwenden ferner das Verwenden der genannten Kanaldaten beim separaten punktweisen Ableiten (S360) in Bezug auf die mehreren Punkte umfasst.

6. Vorrichtung nach Anspruch 4, ferner konfiguriert zum Kombinieren (S427) der Schätzungen und der Ableitungen Punkt-für-Punkt für die genannte Vielzahl von Punkten.

7. Vorrichtung nach Anspruch 6, wobei das genannte Kombinieren das Multiplizieren der genannten Schätzungen mit den genannten Ableitungen Punkt-für-Punkt für die genannte Vielzahl von Punkten (146) umfasst.

8. Vorrichtung nach Anspruch 6, wobei das genannte Kombinieren jeweilige Werte ergibt, wobei die genannte Vorrichtung ferner konfiguriert ist zur Schwellenwertbildung (S428) der genannten Werte, wobei die Ausgabe der genannten Schwellenwertbildung die genannten Mikroverkalkungen räumlich identifiziert.

9. Vorrichtung nach Anspruch 1, wobei das genannte Schätzen das räumliche Zusammensetzen eines Kohärenzfaktors (204) durch Summieren, über mehrere Sendestrahlenbündel, einer Funktion der genannten Daten in Bezug auf: a) ein gegebenes Empfangsstrahlenbündel und b) eine gegebene räumliche Tiefe oder Zeit umfasst.

10. Vorrichtung nach Anspruch 9, wobei das genannte Schätzen (306) ferner das Summieren der genannten Funktion über die genannten Kanäle umfasst.

11. Vorrichtung nach Anspruch 1, ferner dafür konfiguriert, dass für einen Datenwert unter den genannten erfassten Kanaldaten, der komplex ist, wobei sein reeller Teil und sein imaginärer Teil beide ungleich null sind, bei Verwendung für das Schätzen und für das Ableiten die genannten Daten bei der genannten Verwendung Strahlformungsverzögerungen (S310) unterzogen wurden.

12. Vorrichtung nach Anspruch 1, wobei das genannte Verwenden umfasst, dass die erfassten Kanaldaten Strahlformungsverzögerungen unterzogen werden.

13. Vorrichtung nach Anspruch 12, wobei die genannte Vorrichtung ferner derartig konfiguriert ist, dass das Schätzen für die verzögerten Daten durch Summieren erfolgt, wodurch eine Strahlformung (145) durchgeführt wird.

14. Vorrichtung nach Anspruch 12, wobei die genannte Vorrichtung ferner derartig konfiguriert ist, dass das Ableiten der verzögerten Daten separat nach Kanal erfolgt.

15. Vorrichtung nach Anspruch 1, wobei die genannte Matrix (210) eine Vielzahl von Eigenwerten hat, wobei die genannten Eigenwerte unter den mehreren Eigenwerten sind, wobei die genannte Dominanz eine Metrik ist, die einen Vergleich zwischen dem genannten Eigenwert und den genannten mehreren Eigenwerten darstellt, wobei die Vorrichtung konfiguriert ist, um die genannte Matrix anhand der genannten erfassten Kanaldaten zu erzeugen, wobei das genannte Ableiten das Berechnen der genannten Eigenwerte umfasst.

16. Vorrichtung nach Anspruch 1, wobei die genannten Kanaldaten nach dem genannten Ableiten komplexe Funkfrequenzkanaldaten sind, auf die Strahlformungsverzögerungen angewendet wurden, wobei das genannte Ableiten das Nehmen einer Konjugat-Transponierten (220) einer Matrix von genannten Kanaldaten umfasst, wobei Einträge der genannten Konjugat-Transponierten nach Kanal variieren.

17. Vorrichtung nach Anspruch 16, wobei das genannte Ableiten Folgendes umfasst:

Bilden einer Produktmatrix, wobei das genannte Bilden das Multiplizieren der genannten Matrix von genannten

Kanaldaten mit der genannten Konjugat-Transponierten umfasst; und
Mittelwertbildung der genannten Produktmatrix über einen Bereich von räumlicher Tiefe (140) oder Zeit, um die genannte Dominanz abzuleiten, die einem gegebenen räumlichen Punkt entspricht.

18. Vorrichtung nach Anspruch 16, wobei das genannte Ableiten Folgendes umfasst:

Bilden einer Produktmatrix, wobei das genannte Bilden das Multiplizieren der genannten Matrix (222) von genannten Kanaldaten mit der genannten Konjugat-Transponierten umfasst; und
Mittelwertbildung der genannten Produktmatrix über mehrere Sendungen.

19. Vorrichtung nach Anspruch 16, konfiguriert, um beim Erzeugen der genannten komplexen Funkfrequenzkanaldaten einen Algorithmus zu verwenden, der retrospektiv fokussierte Sendestrahlenbündel neu erzeugt.

20. Vorrichtung nach Anspruch 1, wobei das genannte Unterscheiden das Entscheiden (S440), basierend auf der Anwendung eines Kohärenzschwellenwerts auf ein Ergebnis der Schätzung, umfasst, dass sich an einem gegebenen räumlichen Punkt eine Mikroverkalkung befindet.

21. Vorrichtung nach Anspruch 20, wobei das genannte Unterscheiden das Prüfen, wenn die Entscheidung eine andere ist als dass sich eine Mikroverkalkung an dem gegebenen räumlichen Punkt befindet, ob das genannte Ergebnis und die genannte abgeleitete Dominanz einen anderen Kohärenzschwellenwert beziehungsweise einen Dominanzschwellenwert einhalten (S444, S446).

22. Vorrichtung nach Anspruch 1, wobei das genannte Erfassen für einen Mikroverkalkungspartikel mit einer räumlichen Auflösung (138) durchgeführt wird, wobei der genannte Partikel kleiner ist als die genannte Auflösung.

23. Vorrichtung nach Anspruch 1, wobei der genannte Hintergrund Körpergewebe (107) ist, in dem sich die genannten Mikroverkalkungen befinden.

24. Computerlesbares Medium, das ein Programm für eine Analyse medizinischer Ultraschallerfassungsdaten verkörpert, wobei das genannten Programm durch einen Prozessor ausführbare Anweisungen aufweist, die die Vorrichtung nach Anspruch 1 veranlassen, die folgenden Aktionen durchzuführen:

Erfassen von Kanaldaten über Ultraschall, der auf mehreren Kanälen empfangen wird;
Verwenden der erfassten Kanaldaten zum Schätzen der Kohärenz der genannten Daten und zum Ableiten der Dominanz eines Eigenwerts (212) einer Kanalkovarianzmatrix; und
Unterscheiden von Mikroverkalkungen vom Hintergrund basierend auf der Schätzung und der abgeleiteten Dominanz.

Revendications

1. Dispositif médical d'analyse de données d'acquisition par ultrasons ayant une pluralité de canaux (108) et configuré pour :

acquérir des données de canal via des ultrasons reçus sur les canaux ;
caractérisé en ce que les données de canal acquises sont utilisées pour estimer une cohérence desdites données et pour déduire une dominance d'une valeur propre d'une matrice de covariance de canal ; et,
sur la base de l'estimation et de la dominance déduite, distinguer des microcalcifications (142) du fond.

2. Dispositif selon la revendication 1, comprenant un affichage (128) et configuré en outre pour afficher, sur ledit affichage, les microcalcifications distinguées dans une vue ultrasonore.

3. Dispositif selon la revendication 2, configuré en outre pour afficher sur ledit affichage lesdites microcalcifications dans une présentation qui, sur la base d'un résultat de ladite distinction, distingue visuellement (S504) lesdites microcalcifications dudit fond.

4. Dispositif selon la revendication 1, ladite utilisation comprenant l'utilisation desdites données (144) pour estimer une cohérence desdites données individuellement par rapport à une pluralité de points spatiaux ayant respectivement

à la fois a) un faisceau de réception associé ; et b) une profondeur spatiale ou un temps.

5. Dispositif selon la revendication 4, ladite utilisation comprenant en outre l'utilisation desdites données de canal dans la déduction (S360) séparément par point par rapport à la pluralité de points.

6. Dispositif selon la revendication 4, configuré en outre pour combiner (S427) les estimations et les déductions point par point pour ladite pluralité de points.

7. Dispositif selon la revendication 6, ladite combinaison comprenant la multiplication desdites estimations par lesdites déductions point par point pour ladite pluralité de points (146).

8. Dispositif selon la revendication 6, ladite combinaison générant des valeurs respectives, ledit dispositif étant en outre configuré pour un seuillage (S428) desdites valeurs, la sortie dudit seuillage identifiant spatialement lesdites microcalcifications.

9. Dispositif selon la revendication 1, ladite estimation comprenant une composition spatiale d'un facteur de cohérence (204) en additionnant, sur plusieurs faisceaux d'émission, une fonction desdites données par rapport à : a) un faisceau de réception donné ; et b) une profondeur spatiale ou un temps donné.

10. Dispositif selon la revendication 9, ladite estimation (306) comprenant en outre l'addition de ladite fonction sur lesdits canaux.

11. Dispositif selon la revendication 1, en outre configuré pour une donnée parmi lesdites données de canal acquises étant complexe, avec ses parties réelle et imaginaire étant toutes deux non nulles, lors de l'utilisation pour l'estimation et pour la déduction, lesdites données, lors de ladite utilisation, ayant été soumises à des retards de formation de faisceau (S310).

12. Dispositif selon la revendication 1, ladite utilisation comprenant la soumission des données de canal acquises à des retards de formation de faisceau.

13. Dispositif selon la revendication 12, ledit dispositif étant en outre configuré de telle sorte que l'estimation fonctionne sur les données retardées par addition, en réalisant ainsi une formation de faisceau (145).

14. Dispositif selon la revendication 12, ledit dispositif étant en outre configuré de telle sorte que la déduction fonctionne sur les données retardées séparément par canal.

15. Dispositif selon la revendication 1, ladite matrice (210) ayant une pluralité de valeurs propres, ladite valeur propre étant parmi la pluralité de valeurs propres, ladite dominance étant une métrique représentant une comparaison entre ladite valeur propre et ladite pluralité de valeurs propres, ledit dispositif étant configuré pour créer ladite matrice à partir desdites données de canal acquises, ladite déduction comprenant le calcul de ladite valeur propre.

16. Dispositif selon la revendication 1, lesdites données de canal étant, lors de ladite déduction, des données de canal radiofréquence complexes auxquelles des retards de formation de faisceau ont été appliqués, ladite déduction comprenant une prise d'une transposée conjuguée (220) d'une matrice desdites données de canal, des entrées de ladite transposée conjuguée variant par canal.

17. Dispositif selon la revendication 16, ladite déduction comprenant les étapes consistant à :

former une matrice de produit, ladite formation comprenant une multiplication de ladite matrice desdites données de canal par ladite transposée conjuguée ; et
calculer la moyenne de ladite matrice de produit sur une plage de profondeur spatiale (140) ou de temps pour déduire ladite dominance correspondant à un point spatial donné.

18. Dispositif selon la revendication 16, ladite déduction comprenant les étapes consistant à :

former une matrice de produit, ladite formation comprenant la multiplication de ladite matrice (222) desdites données de canal par ladite transposée conjuguée ; et
calculer la moyenne de ladite matrice de produit sur plusieurs transmissions.

19. Dispositif selon la revendication 16, configuré pour, lors de la création desdites données de canal radiofréquence complexes, utiliser un algorithme qui recrée de manière rétrospective des faisceaux d'émission focalisés.

20. Dispositif selon la revendication 1, dans lequel ladite distinction comprenant la décision (S440), sur la base d'une application d'un seuil de cohérence au résultat de l'estimation, qu'une microcalcification réside en un point spatial donné.

21. Dispositif selon la revendication 20, ladite distinction comprenant une vérification, si la décision est autre qu'une microcalcification réside au point spatial donné, que ledit résultat et ladite dominance déduite satisfont ou non respectivement un autre seuil de cohérence et un seuil de dominance (S444, S446).

22. Dispositif selon la revendication 1, ladite acquisition pour une particule de microcalcification étant réalisée avec une résolution spatiale (138), ladite particule étant inférieure à ladite résolution.

23. Dispositif selon la revendication 1, ledit fond étant un tissu corporel (107) dans lequel résident lesdites microcalcifications.

24. Support lisible par ordinateur incorporant un programme médical d'analyse de données d'acquisition par ultrasons, ledit programme ayant des instructions exécutables par un processeur pour amener le dispositif selon la revendication 1 à accomplir les actes suivants :

acquérir des données de canal via des ultrasons reçus sur plusieurs canaux ;
utiliser les données de canal acquises pour estimer une cohérence desdites données et pour déduire une dominance d'une valeur propre (212) d'une matrice de covariance de canal ; et,
sur la base de l'estimation et de la dominance déduite, distinguer des microcalcifications d'un fond.

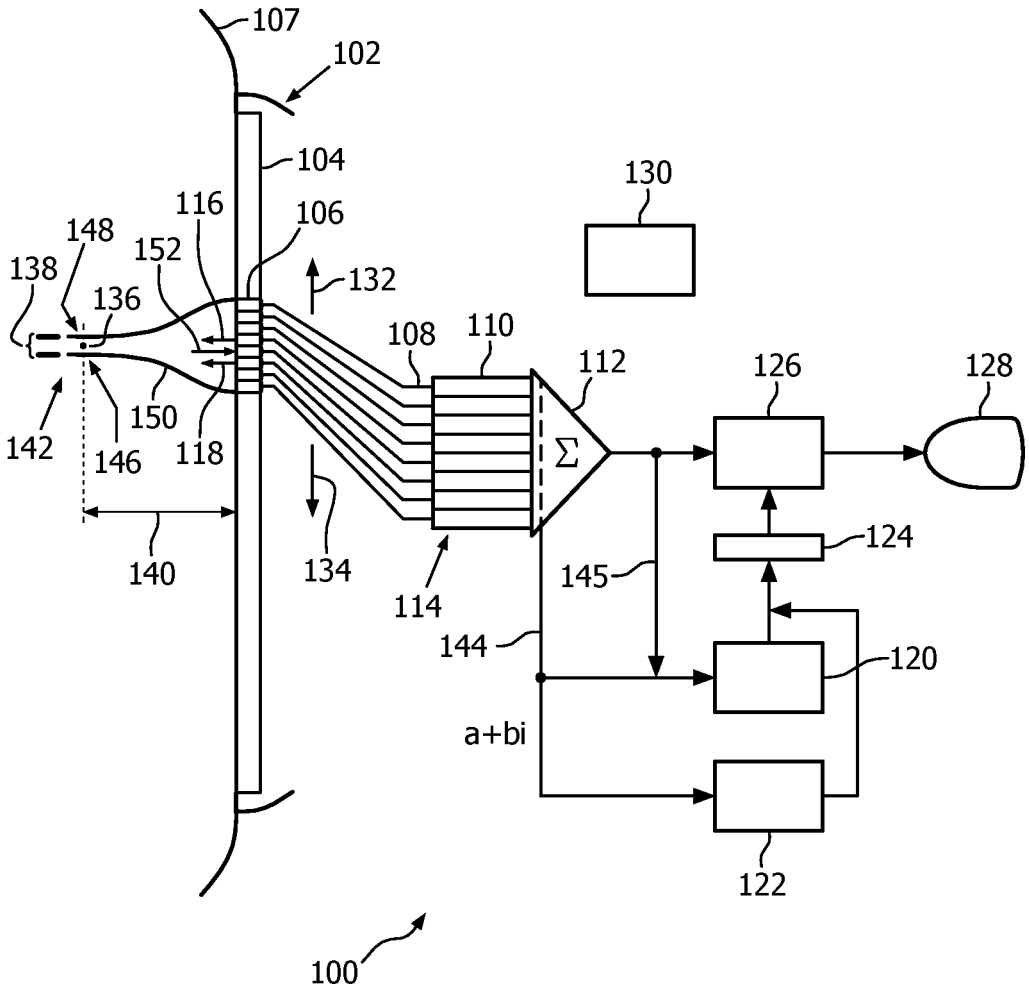
107
102
104
130
116
106
148
152
138
136
132
108
110
112
126
128
142
150
146
118
140
134
114
145
124
144
120
a+bi
122
100
Σ

FIG. 1

$$CF(m,rx) \equiv \frac{\sum_{tx=rx-\Delta}^{rx+\Delta} \left| \sum_{n=1}^{N} S(m,n,tx,rx) \right|^2}{\sum_{tx=rx-\Delta}^{rx+\Delta} N \sum_{n=1}^{N} \left| S(m,n,tx,rx) \right|^2} \quad \text{(definition 1)}$$

204, 206, 208

$$R(m,rx) \equiv \frac{1}{2d+1} \sum_{p=m-d}^{m+d} s(p,rx) s^H(p,rx) \quad \text{(definition 2)}$$

210, 214, 220, 222, 230

$$\text{where} \quad s(p,rx) = \begin{bmatrix} S(p,1,rx,rx) \\ S(p,2,rx,rx) \\ \vdots \\ S(p,N,rx,rx) \end{bmatrix} \quad \text{(definition 3)}$$

$$Tr\{R(m,rx)\} \equiv \sum_{i=1}^{N} R_{ii}(m,rx) = \sum_{i=1}^{N} \gamma_i(m,rx) \quad \text{(definition 4)}$$

212

$$ev_d(m,rx) \equiv \frac{1}{1 - \frac{\gamma_1(m,rx)}{Tr\{R(m,rx)\}}} \quad \text{(definition 5)}$$

216, 218, 228

$$R(m,rx) \equiv \frac{1}{(2d+1)(2g+1)} \sum_{p=m-d}^{m+d} \sum_{tx=rx=g}^{rx+g} s(p,tx,rx) s^H(p,tx,rx) \quad \text{(definition 6)}$$

224, 226

$$\text{where} \quad s(p,tx,rx) = \begin{bmatrix} S(p,1,tx,rx) \\ S(p,2,tx,rx) \\ \vdots \\ S(p,N,tx,rx) \end{bmatrix} \quad \text{(definition 7)}$$

FIG. 2

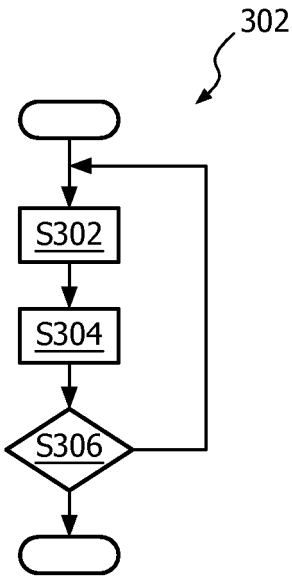

FIG. 3A

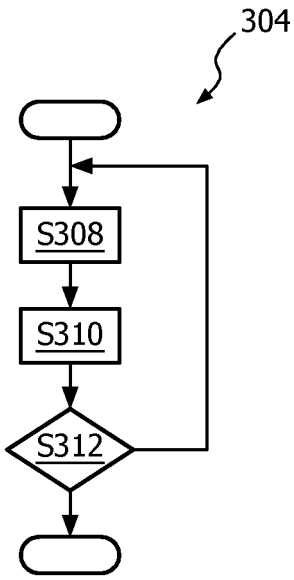

FIG. 3B

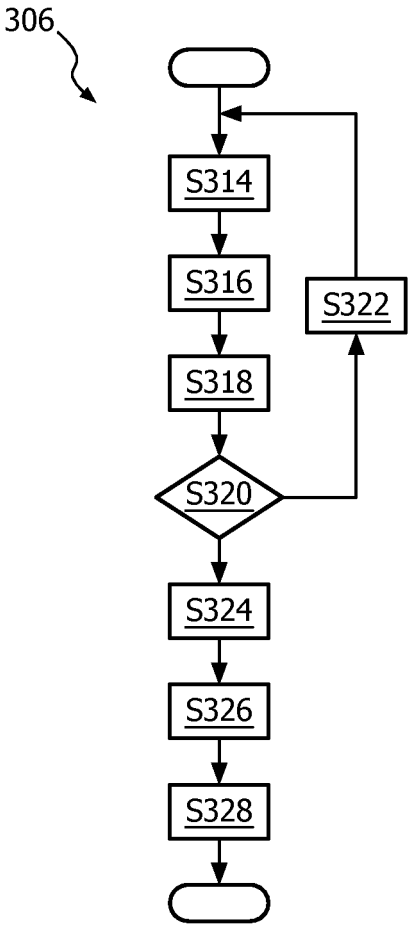
306
S314
S316
S318
S320
S322
S324
S326
S328

FIG. 3C

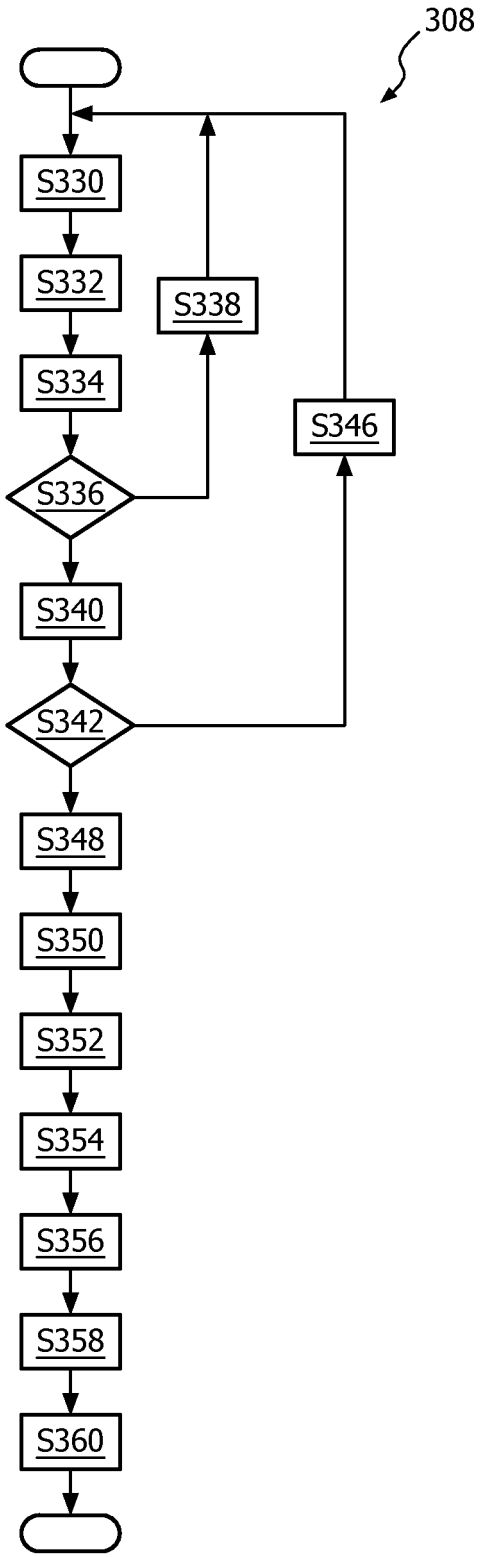
308
S330
S332
S334
S336
S338
S340
S342
S346
S348
S350
S352
S354
S356
S358
S360

FIG. 3D

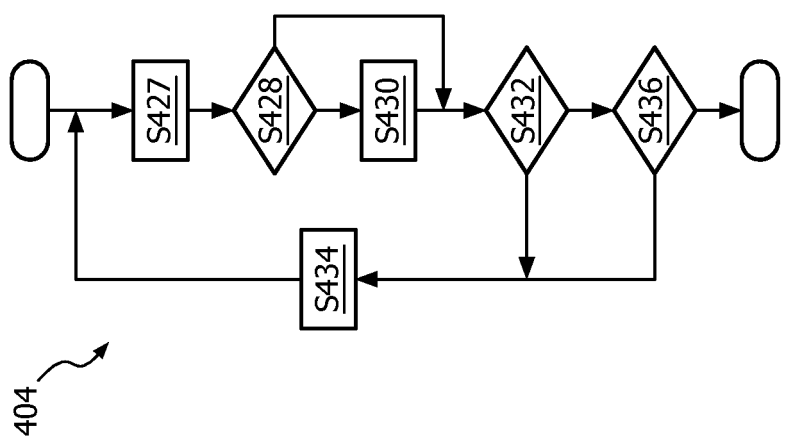
S427
S428
S430
S432
S436
S434
404

FIG. 4B

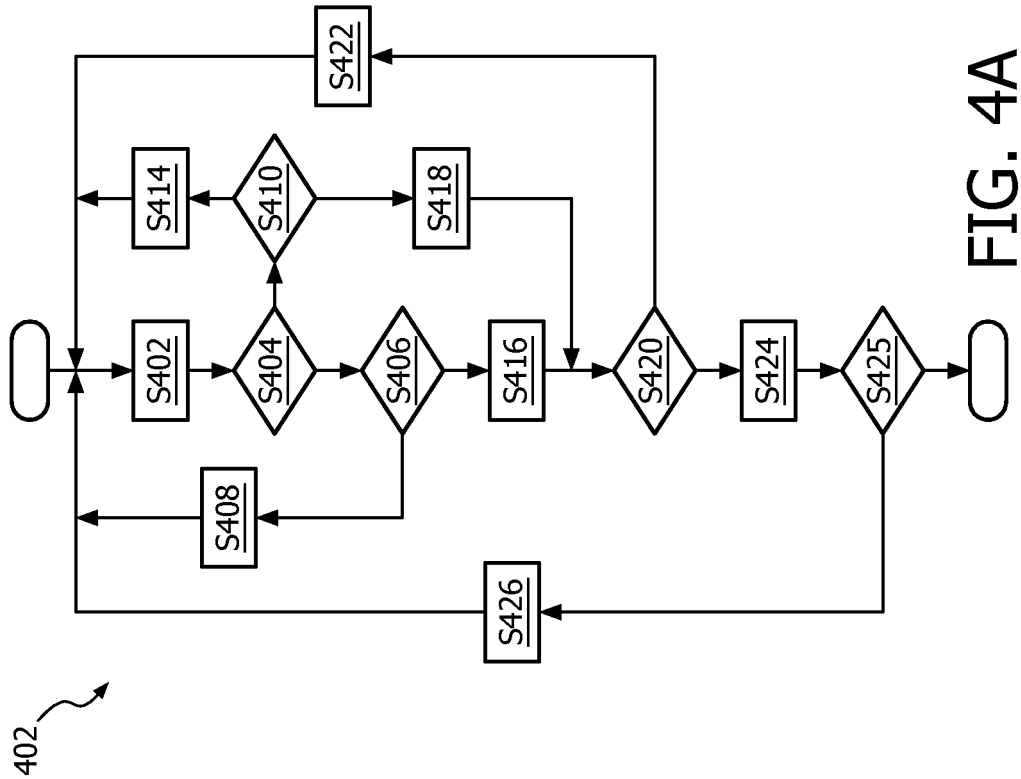
S422
S414
S410
S418
S402
S404
S406
S416
S420
S424
S425
S408
S426
402

FIG. 4A

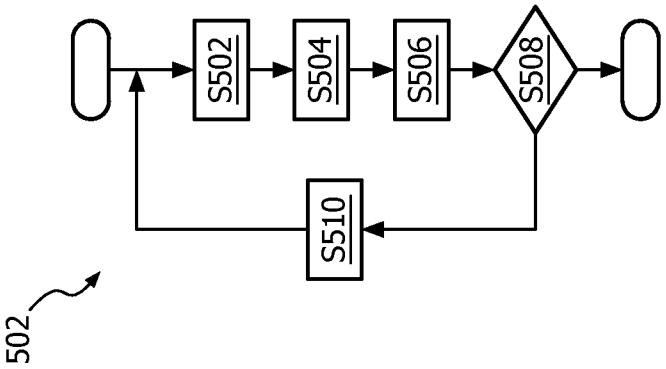
S502
S504
S506
S508
S510
502

FIG. 5

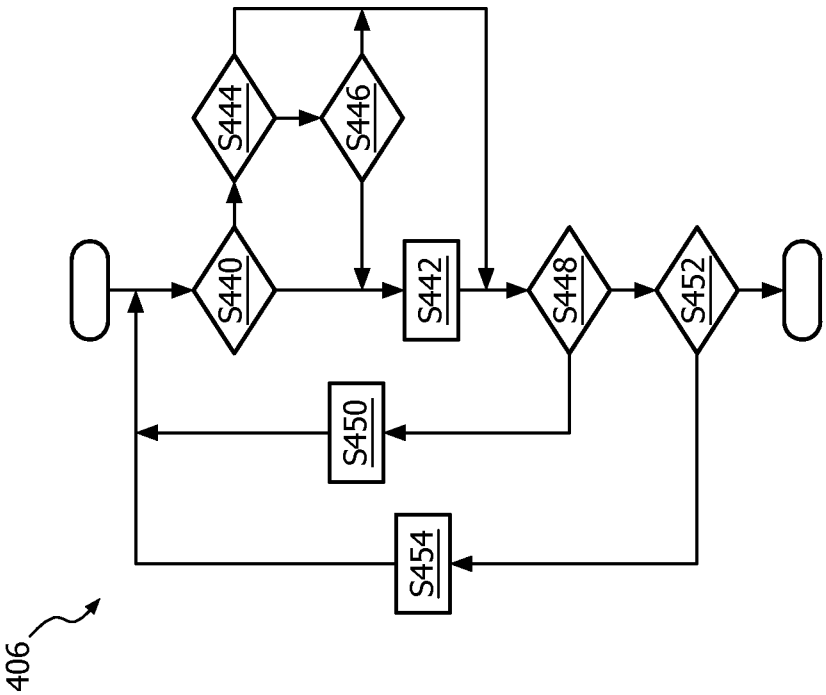
S440
S442
S444
S446
S448
S450
S452
S454
406

FIG. 4C

REFERENCES CITED IN THE DESCRIPTION

This list of references cited by the applicant is for the reader's convenience only. It does not form part of the European patent document. Even though great care has been taken in compiling the references, errors or omissions cannot be excluded and the EPO disclaims all liability in this regard.

Patent documents cited in the description

- US 20060171573 A1 **[0004]**
- US 8317712 B, Burcher **[0033]**

Non-patent literature cited in the description

- **I. CHRISTOYIANNI.** Computer aided diagnoses of breast cancer in digitized mammograms. *Computerized Medical Imaging and Graphics,* 01 September 2002, vol. 26 (5), ISSN 0895-6111, 309-319 **[0003]**
- Ultrasonic computed tomography reconstruction of the attenuation coefficient using a linear array. **SHENG-WEN HUANG et al.** IEEE Transactions on ultrasonics, ferroelectrics and frequency control. IEEE, 01 November 2005, vol. 52, 2011-2022 **[0007]**
- **R. MALLART ; M. FINK.** Adaptive focusing in scattering media through sound-speed inhomogeneities: The van Cittert Zernike approach and focusing criterion. *J. Acoust. Soc. Am.,* 1994, vol. 96 (6), 3721-3732 **[0008]**
- **G. MONTALDO ; M. TANTER ; J. BERCOFF ; N. BENECH ; M. FINK.** Coherent plane-wave compounding for very high frame rate ultrasonography and transient elastography. *IEEE Trans. Ultrason. Ferroelectr. Freq. Control,* 2009, vol. 56 (3), 489-506 **[0033]**
- **J. A. JENSEN ; S. I. NIKOLOV ; K. L. GAMMELMARK ; M. H. PEDERSEN.** Synthetic aperture ultrasound imaging. *Ultrasonics,* 2006, vol. 44, e5-e15 **[0033]**
- **J.R. ROBERT ; M. FINK.** Green's function estimation in speckle using the decomposition of the time reversal operator: Application to aberration correction in medical imaging. *J. Acoust. Soc. Am.,* 2008, vol. 123 (2), 866-877 **[0035]**

专利名称(译)	超声微钙化检测的波束成形技术		
公开(公告)号	EP2976017B1	公开(公告)日	2019-10-02
申请号	EP2014713923	申请日	2014-03-12
[标]申请(专利权)人(译)	皇家飞利浦电子股份有限公司		
申请(专利权)人(译)	皇家飞利浦N.V.		
当前申请(专利权)人(译)	皇家飞利浦N.V.		
[标]发明人	ROBERT JEAN LUC HUANG SHENG WEN RADULESCU EMIL GEORGE VIGNON FRANCOIS GUY GERARD MARIE ERKAMP RAMON QUIDO		
发明人	ROBERT, JEAN-LUC HUANG, SHENG-WEN RADULESCU, EMIL GEORGE VIGNON, FRANCOIS GUY GERARD MARIE ERKAMP, RAMON QUIDO		
IPC分类号	A61B8/08		
代理机构(译)	STEFFEN，THOMAS		
优先权	61/803634 2013-03-20 US 61/907022 2013-11-21 US		
其他公开文献	EP2976017A1		
外部链接	Espacenet		

摘要(译)

医用超声获取数据分析设备通过在通道上接收的超声来获取通道数据（144），使用获取的通道数据来估计数据相干性，并得出通道协方差矩阵的特征值的优势度，并基于该估计值和优势，将微钙化（142）与背景区分开。然后可以通过加亮，着色，注释等在屏幕上使微钙化在视觉上可区分。通过估计可操作的信道数据可能已经经历了波束形成延迟，并且可以在估计中执行的波束形成过程中求和。在估计和推导中，两个场点到场点都可以将多个串行发送（116、118）用于每个场点。在一个实施例中，将估计和推导的结果逐点相乘并提交给阈值。